Supplemental Materials – Pose Estimation from Line Correspondences: A Complete Analysis and A Series of Solutions

Chi Xu, Lilian Zhang, Li Cheng, Reinhard Koch

I. Proofs of lemmas in Sec. III-D

Lemma 1: When $\mathbf{v}_0^w \perp \mathbf{v}_1^w$, $\mathbf{v}_0^w \perp \mathbf{v}_2^w$ and $\mathbf{v}_1^w \perp \mathbf{v}_2^w$, the symmetric kernels in Eq.(12) are exactly the 4 possible candidates given in Eq.(13).

Proof: As $\mathbf{v}_0^w \perp \mathbf{v}_1^w$, $\mathbf{v}_0^w \perp \mathbf{v}_2^w$ and $\mathbf{v}_1^w \perp \mathbf{v}_2^w$, we can construct $\mathbf{V}^w$ and $\mathbf{V}^c$ as orthogonal matrices. To ensure $\mathbf{\Omega}$ be a rotation matrix, we need $\det(\mathbf{\Omega}) = 1$ and $\mathbf{\Omega}^T\mathbf{\Omega} = I$.

For any $\mathbf{M}$ from the possible combinations defined in Eq.(13), we have $\det(\mathbf{\Omega}) = 1$ and

$$\begin{aligned}\mathbf{\Omega}^T\mathbf{\Omega} &= \left(\mathbf{V}^c\mathbf{M}(\mathbf{V}^w)^{-1}\right)^T\left(\mathbf{V}^c\mathbf{M}(\mathbf{V}^w)^{-1}\right)\\ &= (\mathbf{V}^w)^{-T}\mathbf{M}^T(\mathbf{V}^c)^T\mathbf{V}^c\mathbf{M}(\mathbf{V}^w)^{-1} = I.\end{aligned}$$

Therefore, the symmetric kernels in this case are those in Eq.(13). ∎

Lemma 2: When $rank(\mathbf{V}^w) = 3$, $\mathbf{v}_0^w \perp \mathbf{v}_1^w$, $\mathbf{v}_0^w \perp \mathbf{v}_2^w$ and $\mathbf{v}_1^w \not\perp \mathbf{v}_2^w$, the symmetric kernel in Eq.(12) belongs to a further reduced set $\mathbf{M} \in \{diag[1,1,1],\ diag[1,-1,-1]\}$.

Proof: According to the Euclidean transform, we have $\mathbf{v}_0^c \perp \mathbf{v}_1^c$, $\mathbf{v}_0^c \perp \mathbf{v}_2^c$, $\mathbf{v}_1^c \not\perp \mathbf{v}_2^c$, and

$$\begin{aligned}\mathbf{\Omega}^T\mathbf{\Omega} &= \left(\mathbf{V}^c\mathbf{M}(\mathbf{V}^w)^{-1}\right)^T\left(\mathbf{V}^c\mathbf{M}(\mathbf{V}^w)^{-1}\right)\\ &= (\mathbf{V}^w)^{-T}\mathbf{M}^T\mathbf{A}\mathbf{M}(\mathbf{V}^w)^{-1},\end{aligned}$$

in which

$$\mathbf{A} = (\mathbf{V}^c)^T\mathbf{V}^c = \begin{bmatrix}1 & 0 & 0\\ 0 & 1 & c\\ 0 & c & 1\end{bmatrix},$$

and $c = (\mathbf{v}_1^c)^T\mathbf{v}_2^c \neq 0$. Let $\mathbf{M} = diag(m_1, m_2, m_3)$, in order to satisfy the constraint $\mathbf{\Omega}^T\mathbf{\Omega} = I$, we have

$$\begin{aligned}&\mathbf{MAM} = \mathbf{V}^{wT}\mathbf{V}^w\\ \Rightarrow &\begin{bmatrix}m_1m_1 & 0 & 0\\ 0 & m_2m_2 & m_2m_3c\\ 0 & m_2m_3c & m_3m_3\end{bmatrix} = \begin{bmatrix}1 & 0 & 0\\ 0 & 1 & c\\ 0 & c & 1\end{bmatrix}\\ &\Rightarrow m_2m_3 = 1.\end{aligned}$$

Therefore, out of the possible combinations in Eq.(13), the options are $diag(1,1,1)$ and $diag(1,-1,-1)$. ∎

Lemma 3: When $rank(\mathbf{V}^w) = 3$, $\mathbf{v}_0^w \not\perp \mathbf{v}_2^w$, $\mathbf{v}_1^w \not\perp \mathbf{v}_2^w$, the symmetric kernel in Eq.(12) can only be $\mathbf{M} = diag[1,1,1]$.

Proof: As $\mathbf{v}_0^w \not\perp \mathbf{v}_2^w$, $\mathbf{v}_1^w \not\perp \mathbf{v}_2^w$, it gives

$$\mathbf{A} = (\mathbf{V}^c)^T\mathbf{V}^c = \begin{bmatrix}1 & a & b\\ a & 1 & c\\ b & c & 1\end{bmatrix},$$

in which $a = (\mathbf{v}_0^c)^T\mathbf{v}_1^c$, $b = (\mathbf{v}_0^c)^T\mathbf{v}_2^c \neq 0$, and $c = (\mathbf{v}_1^c)^T\mathbf{v}_2^c \neq 0$. In order to meet the constraint $\mathbf{\Omega}^T\mathbf{\Omega} = I$, we have

$$\begin{aligned}&\mathbf{MAM} = \mathbf{V}^{wT}\mathbf{V}^w\\ \Rightarrow &\begin{bmatrix}m_1m_1 & m_1m_2a & m_1m_3b\\ m_2m_1a & m_2m_2 & m_2m_3c\\ m_3m_1b & m_3m_2c & m_3m_3\end{bmatrix} = \begin{bmatrix}1 & a & b\\ a & 1 & c\\ b & c & 1\end{bmatrix}\\ &\Rightarrow \begin{cases} m_1m_2 = \begin{cases}1 & if\ a \neq 0\\ \pm 1 & if\ a = 0\end{cases}\\ m_1m_3 = m_2m_3 = 1,\end{cases}\end{aligned}$$

Therefore, from the possible combinations in Eq.(13), the only feasible kernel is $\mathbf{M} = diag(1,1,1)$. ∎

Lemma 4: When $rank(\mathbf{V}^w) = 2$ and $\mathbf{v}_0^w \parallel \mathbf{v}_1^w \parallel \mathbf{v}_2^w$, two full rank matrices can be constructed as:

$$\hat{\mathbf{V}}^c = [\mathbf{v}_0^c \times \mathbf{v}_1^c,\ \mathbf{v}_0^c,\ \mathbf{v}_1^c],\quad \hat{\mathbf{V}}^w = [\mathbf{v}_0^w \times \mathbf{v}_1^w,\ \mathbf{v}_0^w,\ \mathbf{v}_1^w],$$

The rotation solution is $\mathbf{R}_w^c = \hat{\mathbf{V}}^c\mathbf{M}(\hat{\mathbf{V}}^w)^{-1}$ with symmetric kernel $\mathbf{M} \in \{diag[1,1,1],\ diag[1,-1,-1]\}$.

Proof: First, find the relationships between $\hat{\mathbf{V}}^c\mathbf{M} = \mathbf{R}_w^c\hat{\mathbf{V}}^w$ and $\mathbf{V}^c\mathbf{M} = \mathbf{R}_w^c\mathbf{V}^w$. Since $rank(\mathbf{V}^w) = 2$ and $\mathbf{v}_0^w \parallel \mathbf{v}_1^w \parallel \mathbf{v}_2^w$, we have

$$\mathbf{v}_2^c = k_0\mathbf{v}_0^c + k_1\mathbf{v}_1^c,\ \mathbf{v}_2^w = k_0\mathbf{v}_0^w + k_1\mathbf{v}_1^w, \tag{29}$$

in which k_0 and k_1 are non-zero coefficients. If $\mathbf{R}_w^c$ is the solution of $\hat{\mathbf{V}}^c\mathbf{M} = \mathbf{R}_w^c\hat{\mathbf{V}}^w$ in which $\mathbf{M}$ is a diagonal matrix as defined in Eq.(11), then according to the definition of $\hat{\mathbf{V}}^c$ and $\hat{\mathbf{V}}^w$, we have

$$m_2\mathbf{v}_0^c = \mathbf{R}_w^c\mathbf{v}_0^w,\ m_3\mathbf{v}_1^c = \mathbf{R}_w^c\mathbf{v}_1^w. \tag{30}$$

Combining Eq.(29) and Eq.(30), yield:

$$\mathbf{v}_2^c = k_0\mathbf{v}_0^c + k_1\mathbf{v}_1^c = \mathbf{R}_w^c(k_0m_2\mathbf{v}_0^w + k_1m_3\mathbf{v}_1^w) \tag{31}$$

When $m_2 = m_3 = \pm 1$, from Eq.(31) we get $\mathbf{v}_2^c = \pm\mathbf{R}_w^c\mathbf{v}_2^w$, i. e. $\mathbf{R}_w^c$ is also a solution of $\mathbf{V}^c\mathbf{M} = \mathbf{R}_w^c\mathbf{V}^w$.

Now, we find the rotation solution of $\hat{\mathbf{V}}^c\mathbf{M} = \mathbf{R}_w^c\hat{\mathbf{V}}^w$. By construction, $rank(\hat{\mathbf{V}}^w) = 3$, there are two sub-cases: $\mathbf{v}_0^w \perp \mathbf{v}_1^w$ or $\mathbf{v}_0^w \not\perp \mathbf{v}_1^w$.

If $\mathbf{v}_0^w \perp \mathbf{v}_1^w$, then the column vectors in $\hat{\mathbf{V}}^w$ are orthogonal. According to Lemma 1, the solution is $\mathbf{R}_w^c = \hat{\mathbf{V}}^c\mathbf{M}(\hat{\mathbf{V}}^w)^{-1}$ with symmetric kernels in Eq.(13). Only when $m_2 = m_3 = \pm 1$, $\mathbf{R}_w^c$ will also be a solution of $\mathbf{V}^c\mathbf{M} = \mathbf{R}_w^c\mathbf{V}^w$. Therefore, the possible symmetric kernels are $diag(1,1,1)$ and $diag(1,-1,-1)$.

If $\mathbf{v}_0^w \not\perp \mathbf{v}_1^w$, then by the construction of $\hat{\mathbf{V}}^w$, Lemma 2 can be applied. Therefore, the rotation solution of $\mathbf{V}^c\mathbf{M} = \mathbf{R}_w^c\mathbf{V}^w$ is $\mathbf{R}_w^c = \hat{\mathbf{V}}^c\mathbf{M}(\hat{\mathbf{V}}^w)^{-1}$ with symmetric kernel $\mathbf{M} \in \{diag[1,1,1],\ diag[1,-1,-1]\}$. ∎

II. P3L SOLUTION OF CLASS A: NO JUNCTION

In Sec.III-E, we presented the solution of $\mathbf{R}_w^c$ for case A.1.a. In this appendix, we present the detailed solution analysis for the rest of cases in class A.

Configuration A.1: $Rank(\mathbf{V}^w) = 3$.

Case A.1.b: $\mathbf{v}_i^w \perp \mathbf{v}_k^w$, $\mathbf{v}_j^w \perp \mathbf{v}_k^w$ and $\mathbf{v}_i^w \not\perp \mathbf{v}_j^w$.

The solution of $\mathbf{R}_w^c$: Without loss of generality, assuming that $\mathbf{v}_0^w \perp \mathbf{v}_1^w$, $\mathbf{v}_0^w \perp \mathbf{v}_2^w$ and $\mathbf{v}_1^w \not\perp \mathbf{v}_2^w$. We form a model coordinate frame in which $\mathbf{v}_0^m$ aligns to Z^m-axis and $\mathbf{v}_1^m$ aligns to X^m-axis. We have $\mathbf{v}_1^m = [1,0,0]^T$ and $\mathbf{v}_2^m = [v_{x2}, v_{y2}, 0]^T$. The constraint equation (3) can be simplified to Eq.(14), in which

$$\begin{cases} \sigma_1 = n'_{x1} \\ \sigma_2 = n'_{y1}\cos\alpha + n'_{z1}\sin\alpha \\ \sigma_4 = v_{y2}\ n'_{y2}\cos\alpha + v_{y2}\ n'_{z2}\sin\alpha + v_{x2}\ n'_{x2} \\ \sigma_5 = v_{x2}\ n'_{y2}\cos\alpha + v_{x2}\ n'_{z2}\sin\alpha - v_{y2}\ n'_{x2}. \end{cases}$$

By substituting $\sin^2\alpha = 1 - \cos^2\alpha$ into Eq.(15), we have

$$u_2\cos^2\alpha + u_1\cos\alpha + u_0 = \sin\alpha(v_1\cos\alpha + v_0).$$

Taking the squares of both sides and denoting $x = \cos\alpha$, a 4-th order polynomial can be constructed as:

$$f(x) = \sum_{k=0}^{4} \delta_k x^k = 0. \tag{32}$$

There exist at most four solutions for $\cos\alpha$. For each solution of α, there exist two solutions for β as Eq.(14) is homogeneous. Therefore, $\mathbf{R}_w^c$ has at most $4 \times 2 = 8$ solutions.

Case A.1.c: $\mathbf{v}_i^w \not\perp \mathbf{v}_k^w$, $\mathbf{v}_j^w \not\perp \mathbf{v}_k^w$.

Two line pairs are not perpendicular ($\mathbf{v}_i^w \not\perp \mathbf{v}_k^w$, $\mathbf{v}_j^w \not\perp \mathbf{v}_k^w$), and the third line pair can be either $\mathbf{v}_i^w \perp \mathbf{v}_j^w$ or $\mathbf{v}_i^w \not\perp \mathbf{v}_j^w$. The general polynomial described in Sec.III-A can be used to solve $\mathbf{R}_w^c$ in this case, and there exist at most eight solutions.

Configuration A.2: $Rank(\mathbf{V}^w) = 2$.

Case A.2.a: $\mathbf{v}_i^w \parallel \mathbf{v}_j^w$ and $\mathbf{v}_i^w \perp \mathbf{v}_k^w$.

The solution of $\mathbf{R}_w^c$: Without loss of generality, by assuming $\mathbf{v}_0^w \perp \mathbf{v}_1^w \parallel \mathbf{v}_2^w$, we form a model coordinate frame in which $\mathbf{v}_0^m$ aligns to Z^m-axis, $\mathbf{v}_1^m$ and $\mathbf{v}_2^m$ are parallel to X^m-axis . We have $\mathbf{v}_1^m = \mathbf{v}_2^m = [1,0,0]^T$. The constraint equation (3) can be simplified to Eq.(14), in which

$$\begin{cases} \sigma_1 = n'_{x1} \\ \sigma_2 = n'_{y1}\cos\alpha + n'_{z1}\sin\alpha \\ \sigma_4 = n'_{x2} \\ \sigma_5 = n'_{y2}\cos\alpha + n'_{z2}\sin\alpha. \end{cases} \tag{33}$$

By substituting Eq.(33) into Eq.(15), we have

$$(n'_{x2}n'_{y1} - n'_{x1}n'_{y2})\cos\alpha + (n'_{x2}n'_{z1} - n'_{x1}n'_{z2})\sin\alpha = 0,$$

from which a linear equation about $x = \tan\alpha$ can be constructed. For the solution of $\tan\alpha$, there exist two symmetric solutions for α. For each solution of α, there exist two symmetric solutions for β as Eq.(14) is homogeneous. Therefore, $\mathbf{R}_w^c$ has at most $2 \times 2 = 4$ solutions.

Case A.2.b: $\mathbf{v}_i^w \parallel \mathbf{v}_j^w$ and $\mathbf{v}_i^w \not\perp \mathbf{v}_k^w$.

The solution of $\mathbf{R}_w^c$: Without loss of generality, by assuming $\mathbf{v}_1^w \parallel \mathbf{v}_2^w$, we form a model coordinate frame in which $\mathbf{v}_0^m$ aligns to Z^m-axis, $\mathbf{v}_1^m$ and $\mathbf{v}_2^m$ are parallel to $X^mO^mZ^m$-plane. We have $\mathbf{v}_1^m = \mathbf{v}_2^m = [v_{x1}, 0, v_{z1}]^T$. The coefficients in constraint equation (3) are

$$\begin{cases} \sigma_1 = v_{x1}\ n'_{x1} \\ \sigma_2 = v_{x1}\ n'_{y1}\cos\alpha + v_{x1}\ n'_{z1}\sin\alpha \\ \sigma_3 = v_{z1}\ n'_{z1}\cos\alpha - \ v_{z1}\ n'_{y1}\sin\alpha \\ \sigma_4 = v_{x1}\ n'_{x2} \\ \sigma_5 = v_{x1}\ n'_{y2}\cos\alpha + v_{x1}\ n'_{z2}\sin\alpha \\ \sigma_6 = v_{z1}\ n'_{z2}\cos\alpha - \ v_{z1}\ n'_{y2}\sin\alpha. \end{cases}$$

By substituting $\sin^2\alpha = 1 - \cos^2\alpha$ into Eq.(5) and rearranging the terms, we have

$$u_1\cos^2\alpha + u_0 = v_1\cos\alpha\sin\alpha.$$

Taking the squares of both sides and denoting $x = \cos^2\alpha$, a 2-nd order polynomial can be constructed as:

$$f(x) = \delta_2 x^2 + \delta_1 x + \delta_0 = 0. \tag{34}$$

There exist at most two solutions for $\cos^2\alpha$ and at most four solutions for α. For each solution of α, only one solution of β can be computed from Eq.(3). Therefore, $\mathbf{R}_w^c$ has at most four solutions.

Case A.2.c: $\mathbf{v}_i^w \not\parallel \mathbf{v}_j^w \not\parallel \mathbf{v}_k^w$.

This case can be divided into two sub-cases: (1) three lines L_0, L_1 and L_2 lie on a plane, and (2) L_0, L_1 and L_2 do not lie on a plane. For the first sub-case, it is equivalent to a P3P problem and can be solved using the P3P polynomial. In the following, we give a general solution for the two sub-cases.

Without loss of generality, we form a model coordinate frame in which $\mathbf{v}_0^m$ aligns to Z^m-axis, $\mathbf{v}_1^m$ and $\mathbf{v}_2^m$ lie on $X^mO^mZ^m$-plane. We have $\mathbf{v}_1^m = [v_{x1}, 0, v_{z1}]^T$ and $\mathbf{v}_2^m = [v_{x2}, 0, v_{z2}]^T$. The coefficients in constraint equation (3) are

$$\begin{cases} \sigma_1 = v_{x1}\ n'_{x1} \\ \sigma_2 = v_{x1}\ n'_{y1}\cos\alpha + v_{x1}\ n'_{z1}\sin\alpha \\ \sigma_3 = v_{z1}\ n'_{z1}\cos\alpha - \ v_{z1}\ n'_{y1}\sin\alpha \\ \sigma_4 = v_{x2}\ n'_{x2} \\ \sigma_5 = v_{x2}\ n'_{y2}\cos\alpha + v_{x2}\ n'_{z2}\sin\alpha \\ \sigma_6 = v_{z2}\ n'_{z2}\cos\alpha - \ v_{z2}\ n'_{y2}\sin\alpha. \end{cases}$$

By substituting $\sin^2\alpha = 1 - \cos^2\alpha$ into Eq.(5) and rearranging the terms, we have

$$u_4\cos^4\alpha + u_2\cos^2\alpha + u_0 = \sin\alpha(u_3\cos^3\alpha + u_1\cos\alpha).$$

Taking the squares of both sides and denoting $x = \cos^2\alpha$, a 4-th order polynomial can be constructed as:

$$f(x) = \sum_{k=0}^{4} \delta_k x^4 = 0.$$

There exist at most four solutions for $\cos^2\alpha$ and at most eight solutions for α. For each solution of α, only one solution of β can be computed from Eq.(3). Therefore, $\mathbf{R}_w^c$ has at most eight solutions.

III. P3L SOLUTION OF CLASS B: JUNCTION

In this appendix, the detailed solution analysis for cases in class B is given.

Configuration B.1: $Rank(\mathbf{V}^w) = 3$.

Case B.1.a: $\mathbf{v}_i^w \perp \mathbf{v}_j^w$, $\mathbf{v}_i^w \perp \mathbf{v}_k^w$ and $\mathbf{v}_j^w \perp \mathbf{v}_k^w$.

Similar to case A.1.a, we form a model coordinate frame and have $\mathbf{v}_1^m = [1,0,0]^T$ and $\mathbf{v}_2^m = [0,1,0]^T$. Since $n'_{z1} = n'_{z2} = 0$, the constraint equation (3) can be simplified to Eq.(14), in which

$$\begin{cases} \sigma_1 = n'_{x1} \\ \sigma_2 = n'_{y1}\cos\alpha \\ \sigma_4 = n'_{y2}\cos\alpha \\ \sigma_5 = -n'_{x2}. \end{cases}$$

By solving Eq.(14), we have

$$n'_{y1}n'_{y2}cos^2\alpha + n'_{x1}n'_{x2} = 0.$$

Let $x = \cos^2\alpha$, a linear equation can be constructed as:

$$f(x) = \delta_1 x + \delta_0 = 0.$$

There exist one solution for $\cos^2\alpha$, two solutions for $\cos\alpha$ and four solutions for α, because there is no constraint on the sign of $\sin\alpha$ which can be $\pm\sqrt{1-\cos^2\alpha}$. For each solution of α, there exist two symmetric solutions of β as Eq.(14) is homogeneous. Therefore, $\mathbf{R}_w^c$ has at most $2\times 2\times 2 = 8$ solutions.

Case B.1.b: $\mathbf{v}_i^w \perp \mathbf{v}_k^w$, $\mathbf{v}_j^w \perp \mathbf{v}_k^w$ and $\mathbf{v}_i^w \not\perp \mathbf{v}_j^w$.

Similar to case A.1.b, we form a model coordinate frame and have $\mathbf{v}_1^m = [1,0,0]^T$ and $\mathbf{v}_2^m = [v_{x2}, v_{y2}, 0]^T$. The constraint equation (3) can be simplified to Eq.(14), in which

$$\begin{cases} \sigma_1 = n'_{x1} \\ \sigma_2 = n'_{y1}\cos\alpha \\ \sigma_4 = v_{y2}\ n'_{y2}\cos\alpha + v_{x2}\ n'_{x2} \\ \sigma_5 = v_{x2}\ n'_{y2}\cos\alpha - v_{y2}\ n'_{x2}. \end{cases}$$

By solving Eq.(14), we have

$$u_2\cos^2\alpha + u_1\cos\alpha + u_0 = 0.$$

Let $x = \cos\alpha$, we have a 2-nd order polynomial:

$$f(x) = \delta_2 x^2 + \delta_1 x + \delta_0 = 0.$$

There exist at most two solutions for $\cos\alpha$ and four solutions for α, because there is no constraint on the sign of $\sin\alpha$ which can be $\pm\sqrt{1-\cos^2\alpha}$. For each solution of α, there exist two solutions for β as Eq.(14) is homogeneous. Therefore, $\mathbf{R}_w^c$ has at most $2\times 2\times 2 = 8$ solutions.

Case B.1.c: $\mathbf{v}_i^w \not\perp \mathbf{v}_k^w$, $\mathbf{v}_j^w \not\perp \mathbf{v}_k^w$.

Similar to case A.1.c, the coefficients in Eq.(3) are

$$\begin{cases} \sigma_1 = v_{y1}\ n'_{y1}\cos\alpha + v_{x1}\ n'_{x1} \\ \sigma_2 = v_{x1}\ n'_{y1}\cos\alpha - v_{y1}\ n'_{x1} \\ \sigma_3 = -v_{z1}\ n'_{y1}\sin\alpha \\ \sigma_4 = v_{y2}\ n'_{y2}\cos\alpha + v_{x2}\ n'_{x2} \\ \sigma_5 = v_{x2}\ n'_{y2}\cos\alpha - v_{y2}\ n'_{x2} \\ \sigma_6 = -v_{z2}\ n'_{y2}\sin\alpha. \end{cases}$$

By solving the equation and rearranging the terms, we have

$$\sum_{k=0}^{4} u_k \cos^k\alpha = 0.$$

There exist at most four solutions for $\cos\alpha$ and eight solutions for α, because there is no constraint on the sign of $\sin\alpha$ which can be $\pm\sqrt{1-\cos^2\alpha}$. Therefore, $\mathbf{R}_w^c$ has at most $4\times 2 = 8$ solutions.

Configuration B.2: $Rank(\mathbf{V}^w) = 2$.

Case B.2.a: $\mathbf{v}_i^w \parallel \mathbf{v}_j^w$ and $\mathbf{v}_i^w \perp \mathbf{v}_k^w$.

There are two sub-cases: (1) three lines pass through a spatial joint point and; (2) the projections of lines meet at a junction. For the first sub-case, since $\mathbf{v}_i^w \parallel \mathbf{v}_j^w$, L_i and L_j must be the same line in space. This sub-case is not of interest because only two distinct lines (L_i and L_k) are observed. We only consider the second sub-case here. Similar to case A.2.a, by assuming $\mathbf{v}_0^w \perp \mathbf{v}_1^w \parallel \mathbf{v}_2^w$, in the model coordinate frame we have $\mathbf{v}_1^m = \mathbf{v}_2^m = [1,0,0]^T$. The constraint equation (3) can be simplified to Eq.(14), in which

$$\begin{cases} \sigma_1 = n'_{x1} \\ \sigma_2 = n'_{y1}\cos\alpha \\ \sigma_4 = n'_{x2} \\ \sigma_5 = n'_{y2}\cos\alpha. \end{cases}$$

By substituting it into Eq.(15), we have

$$(n'_{x2}n'_{y1} - n'_{x1}n'_{y2})\cos\alpha = 0.$$

Since the projections of lines meet at a junction, the projection planes Π_1 and Π_2 are not parallel (i. e. $n'_{x2}n'_{y1} - n'_{x1}n'_{y2} \neq 0$), which yields $\cos\alpha = 0$. From Eq.(14), we get $\cos\beta = 0$. There is no constraint on the sign of $\sin\alpha$ and $\sin\beta$. Hence, there exist two solutions of α and two solutions of β (either 0 or π), respectively. $\mathbf{R}_w^c$ has at most $2\times 2 = 4$ solutions.

Case B.2.b: $\mathbf{v}_i^w \parallel \mathbf{v}_j^w$ and $\mathbf{v}_i^w \not\perp \mathbf{v}_k^w$.

Again, there are two sub-cases: (1) three lines pass through a spatial joint point and; (2) the projections of lines meet at a junction. Only the second sub-case is of interest here. Similar to case A.2.b, by assuming $\mathbf{v}_0^w \not\perp \mathbf{v}_1^w \parallel \mathbf{v}_2^w$, in the model coordinate frame we have $\mathbf{v}_1^m = \mathbf{v}_2^m = [v_{x1}, 0, v_{z1}]^T$. The coefficients in constraint equation (3) are

$$\begin{cases} \sigma_1 = v_{x1}\ n'_{x1} \\ \sigma_2 = v_{x1}\ n'_{y1}\cos\alpha \\ \sigma_3 = -\ v_{z1}\ n'_{y1}\sin\alpha \\ \sigma_4 = v_{x1}\ n'_{x2} \\ \sigma_5 = v_{x1}\ n'_{y2}\cos\alpha \\ \sigma_6 = -\ v_{z1}\ n'_{y2}\sin\alpha. \end{cases}$$

By substituting $\sin^2\alpha = 1-\cos^2\alpha$ into Eq.(5) and rearranging the terms, we have

$$u_2\cos^4\alpha + u_1\cos^2\alpha + u_0 = 0.$$

Denoting $x = \cos^2\alpha$, a 2-nd order polynomial can be constructed as:

$$f(x) = \delta_2 x^2 + \delta_1 x + \delta_0 = 0.$$

There exist at most two solutions for $\cos^2\alpha$ and at most four solutions for α. For each solution of α, only one solution of β can be computed from Eq.(3). Therefore, $\mathbf{R}_w^c$ has at most four solutions.

Case B.2.c: $\mathbf{v}_i^w \nparallel \mathbf{v}_j^w \nparallel \mathbf{v}_k^w$.

Similar to case A.2.c, we form a model coordinate frame and the coefficients in constraint equation (3) are

$$\begin{cases} \sigma_1 = v_{x1}\ n'_{x1} \\ \sigma_2 = v_{x1}\ n'_{y1}\cos\alpha \\ \sigma_3 = -\ v_{z1}\ n'_{y1}\sin\alpha \\ \sigma_4 = v_{x2}\ n'_{x2} \\ \sigma_5 = v_{x2}\ n'_{y2}\cos\alpha \\ \sigma_6 = -\ v_{z2}\ n'_{y2}\sin\alpha. \end{cases}$$

By solving the equation and rearranging the terms, we have

$$u_2\cos^4\alpha + u_1\cos^2\alpha + u_0 = 0.$$

Let $x = \cos^2\alpha$, we have a 2-nd order polynomial:

$$f(x) = \delta_2 x^2 + \delta_1 x + \delta_0 = 0.$$

There exist at most two solutions for $\cos^2\alpha$, four solutions for $\cos\alpha$ and eight solutions for α, because there is no constraint on the sign of $\sin\alpha$ which can be $\pm\sqrt{1-\cos^2\alpha}$. Therefore, $\mathbf{R}_w^c$ has at most $2\times 2\times 2 = 8$ solutions.

IV. Pseudo-code

Algorithm 1 ASPnL

```
divide line set into n − 2 triplets
for each triplet do
    compute f_i(x) using 2D/3D correspondences
F' ← Σ_{i=1}^{n−2} f_i(x) f_i'(x) = 0
compute roots of polynomial F'
for j = 1 ··· m do        ▷ m: number of real roots of F'
    compute rotation R_w^c(j)
    refine R_w^c(j)
    E_or(j) ← Σ_{i=1}^{n} (n_i^{cT} R_w^c v_i^w)^2
j* ← arg min E_or(j)
R_w^{c*} ← R_w^c(j*)
compute t* using R_w^{c*}
```

Algorithm 2 LPnL_DLT_LS

```
parametrize R and T as x
derive linear system M x = 0
x ← solve M x = 0 using least square solver
R_w^c, t ← x
```

V. Dimension of Effective Null Space

In this paper, we follow the work of Lepetit et al. [5] where the dimension of effective null pace is set as 4. For the PnL problem, we have a similar observation to that of the PnP problem: given perfect data without noise, the number of null eigen vector will be exactly one for perspective camera; when the focal length increases and the camera becomes close to orthographic camera, all its 4 smallest eigenvalues approach zero. When the inputs are noisy, the smallest eigenvalues are tiny but not zero.

Besides, we measure the contributions of eigen vectors to the solution, and the result suggests that it is suitable to set the size of effective null space as 4. Let the eigen vectors of $\mathbf{M^TM}$ be $\{\mathbf{V}_i\}$ ($i = 1\cdots 12$, and their corresponding eigenvalues are sorted in increasing order), the ground-truth solution $\mathbf{x}$ can be expressed as a linear combination of the eigen vectors, $\mathbf{x} = \sum_{i=1}^{12}\lambda_i\mathbf{V}_i$. The more $\mathbf{V}_i$ contributes to the solution, the larger $|\lambda_i|$ is. We measure the contribution of i^{th} eigen vector as $\frac{|\lambda_i|}{\sum_{i=1}^{12}|\lambda_i|}$, and the result is shown in

Algorithm 3 LPnL_DLT_ENull

```
parametrize R and T as x
derive linear system M x = 0
x ← solve M x = 0 using ENull solver
R_w^c, t ← x
```

Algorithm 4 LPnL_Bar_LS

```
express lines using barycentric coordinates
parametrize control points {C_j} as x
derive linear system M x = 0
x ← solve M x = 0 using least square solver
{C_j} ← x
compute R_w^c and t using {C_j}
```

Algorithm 5 LPnL_Bar_ENull

```
express lines using barycentric coordinates
parametrize control points {C_j} as x
derive linear system M x = 0
x ← solve M x = 0 using ENull solver
{C_j} ← x
compute R_w^c and t using {C_j}
```

Algorithm 6 RLPnL_LS

```
init W as identity matrix    ▷ W := diag(··· w_i, w_i ···)
express lines using barycentric coordinates
parametrize control points {C_j} as x
derive linear system M x = 0
repeat
    x ← solve W M x = 0 using least square solver
    for i = 1 ··· n do                    ▷ update W
        compute residual ε_i using x
        if ε_i ≤ τ* then
            w_i = 1;
        else
            w_i = 0;
until ||W M x||^2 converges, or the loop reaches max number of iterations.
{C_j} ← x
compute R_w^c and t using {C_j}
```

Algorithm 7 RLPnL_ENull

init $\mathbf{W}$ as identity matrix ▷ $\mathbf{W} := diag(\cdots w_i, w_i \cdots)$
express lines using barycentric coordinates
parametrize control points $\{\mathbf{C}_j\}$ as $\mathbf{x}$
derive linear system $\mathbf{M}\,\mathbf{x} = \mathbf{0}$
repeat
  $\mathbf{x} \leftarrow$ solve $\mathbf{W}\,\mathbf{M}\,\mathbf{x} = \mathbf{0}$ using **ENull** solver
  for $i = 1 \cdots n$ **do** ▷ update $\mathbf{W}$
    compute residual ϵ_i using $\mathbf{x}$
    if $\epsilon_i \leq \tau^*$ **then**
      $w_i = 1$;
    else
      $w_i = 0$;
until $||\mathbf{W}\,\mathbf{M}\,\mathbf{x}||^2$ converges, **or** the loop reaches max number of iterations.
$\{\mathbf{C}_j\} \leftarrow \mathbf{x}$
compute $\mathbf{R}_w^c$ and $\mathbf{t}$ using $\{\mathbf{C}_j\}$

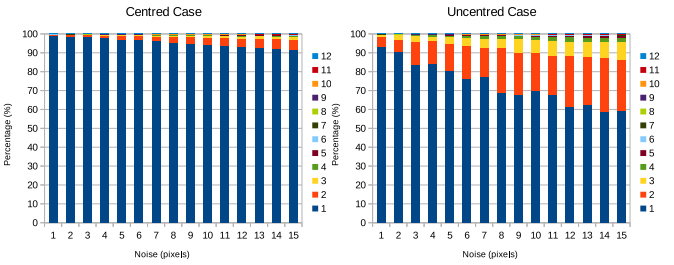

Fig. 9

THE CONTRIBUTIONS OF 12 EIGEN VECTORS ARE PLOTTED AS A FUNCTION OF IMAGE NOISE FROM 1 TO 15 PIXELS BY TAKING AVERAGE OF 100 SYNTHETIC TRIALS. ON THE LEFT IS THE CENTRED CASE, AND ON THE RIGHT IS THE UNCENTRED CASE. THE EIGENVALUES ARE SORTED IN INCREASING ORDER. THE NUMBER OF LINES IS 6.

Fig.9. The higher the noise level is, the higher the dimension of effective null space is. The uncentred case requires more eigen vectors than the centred case. We observe that, in the uncentred case with up to 15 pixels random noise, the first 4 eigen vectors contribute more than 98% to the solution, and it suggests that 4 eigen vectors are sufficient to provide a good approximate $\overline{\mathbf{x}} = \sum_{i=1}^{4} \lambda_i \mathbf{V}_i$. Therefore we chose the dimension of effective null space as 4.

VI. CAMERA POSE REFINEMENT

Kneip et al. [28] proposed a geometrically optimal quaternion-based formulation for generalized PnP problem. In [28], the form of energy function is $s^T M\, s$ where the unknown s contains all quadratic monomials in the quaternion parameters. The terms of s are then expressed as Cayley parameters, and a single Newton step is performed for root polishing.

The derivation of [28] is very different from ours as it aims at the PnP problem, but its energy function shares the same form as that of ours, i.e. a 4th order function with 3 unknown Cayley parameters. Therefore we extend the root polishing method of [28] by replacing its energy function with our PnL energy function. The primary difference lies in that we use Newton method for optimization, but [28] performs a single Newton step for root polishing. As can be seen in Table II, when the perturbation from the initial to the ground-truth is small (e.g. 1 degree), the single Newton step performs the same as that of ours. When the perturbation reaches 10 degrees, ours achieves better accuracy.

perturbation (degrees)	rotation error (degrees)	
	ours	single Newton step
1	0.17	0.17
5	0.17	0.22
10	0.18	0.57

TABLE II

"SINGLE NEWTON STEP" DENOTES THE ROOT POLISHING METHOD EXTENDED FROM [28]. THE NUMBER OF LINES 20, NOISE LEVEL 5 PIXELS, AND EACH VALUE AVERAGES 500 SYNTHETIC TRIALS.

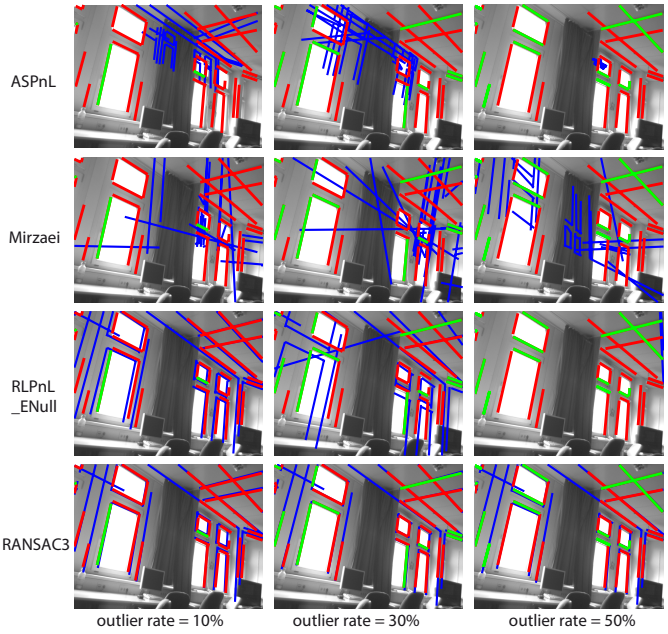

Fig. 10

PERFORMANCE EVALUATION ON REAL IMAGE WHEN OUTLIERS EXIST. THE EXPERIMENTAL RESULTS ILLUSTRATE THE COMPARED PNL SOLUTIONS FOR REAL IMAGES WHEN THE OUTLIER RATE VARIES FROM 10% TO 50%. THE RED LINES ARE THE GIVEN INLIER 2D LINE SEGMENTS. THE GREEN LINES ARE THE OUTLIERS WHOSE CORRESPONDING 3D LINES ARE RANDOMLY GENERATED. THE BLUE LINES ARE THE PROJECTION OF THE 3D LINE MODEL USING THE ESTIMATED CAMERA POSE.

VII. EXPERIMENTS WITH REAL IMAGES

To test the performance of the compared methods when outliers exist in the line set, we choose a few image line segment as outliers and randomly generate their corresponding 3D lines based on the outlier rate which varies from 10% to 50%. From Fig.10, it can be seen that neither **ASPnL** nor **Mirzaei** are robust to outliers. **RLPnL_ENull** has better

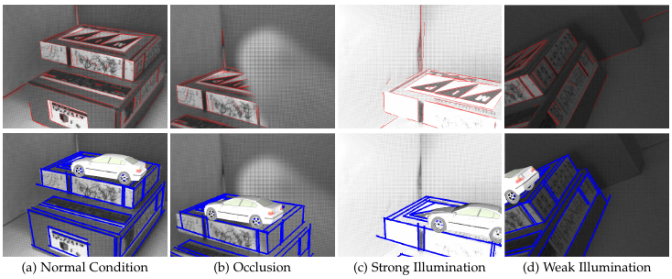

Fig. 11
DEMONSTRATION OF THE AR SYSTEM RUNNING IN REAL-TIME UNDER THE CHALLENGE OF IMAGE OCCLUSIONS AND ILLUMINATION VARIATIONS. THE FIRST ROW SHOWS THE INPUT IMAGES WITH EXTRACTED LINES AND THE SECOND ROW SHOWS THE AUGMENTED IMAGES WITH THE IMPOSED BOX AND CAR MODEL.

performance than those of **ASPnL** and **Mirzaei** when outliers exist. As expected, **RANSAC3** has the best performance which successfully estimates the camera pose even when outlier rate reaches 50%.

To demonstrate the performance of the proposed algorithm in real time applications, we apply it into an augmented reality system. A set of key frames of the scene is grabbed from various view points in advance. Before running the AR system, we apply the SBA algorithm [43] to reconstruct the scene. We employ the **ASPnL** algorithm to estimate the camera pose based on the 2D/3D correspondences. Then the virtual object, e.g. a car model, is superimposed into images using the estimated camera pose. In Fig.11, we demonstrate some snapshots of the AR system running in real-time. The counterpart video is produced from the captured images and the augmented images during the AR system running phase. It can be seen that the system can run smoothly with a hand-held camera. The tracking process is robust to image occlusions and illumination variations.